University of Reading

Structure determination, magnetic and optical properties of a new chromium(II) thioantimonate, [Cr((NH2CH2CH2)(3)N)]Sb4S7

Article

Accepted Version

Powell, A. V., Lees, R.J.E. and Chippindale, A.M. ORCID: https://orcid.org/0000-0002-5918-8701 (2008) Structure determination, magnetic and optical properties of a new chromium(II) thioantimonate, [Cr((NH2CH2CH2)(3)N)]Sb4S7. Journal of Physics and Chemistry of Solids, 69 (4). pp. 1000-1006. ISSN 0022-3697 doi: 10.1016/j.jpcs.2007.11.014 Available at https://centaur.reading.ac.uk/11563/

It is advisable to refer to the publisher's version if you intend to cite from the work. See Guidance on citing.

To link to this article DOI: http://dx.doi.org/10.1016/j.jpcs.2007.11.014

Publisher: Elsevier

All outputs in CentAUR are protected by Intellectual Property Rights law, including copyright law. Copyright and IPR is retained by the creators or other copyright holders. Terms and conditions for use of this material are defined in the End User Agreement.

University of Reading

www.reading.ac.uk/centaur

CentAUR

Central Archive at the University of Reading

Reading's research outputs online

Structure Determination, Magnetic and Optical Properties of a New Chromium(II) Thioantimonate, $[Cr((NH_2CH_2CH_2)_3N)]Sb_4S_7$

Anthony V. Powell*[a], Rachel J.E. Lees[a] and Ann M. Chippindale[b]

[a]*Department of Chemistry, Heriot-Watt University, Edinburgh EH14 4AS, UK*

[b]*Department of Chemistry, The University of Reading, Whiteknights, Reading RG6 6AD, UK*

Correspondence to:
Dr A.V. Powell
Department of Chemistry
Heriot-Watt University
Edinburgh EH14 4AS
UK
Fax: +44 (0)131 451 3180
E-mail: a.v.powell@hw.ac.uk

Abstract

The chromium(II) antimony(III) sulphide, $[Cr((NH_2CH_2CH_2)_3N)]Sb_4S_7$, was synthesised under solvothermal conditions from the reaction of Sb_2S_3, Cr and S dissolved in tris(2-aminoethyl)amine (tren) at 438K. The products were characterised by single-crystal X-ray diffraction, elemental analysis, SQUID magnetrometry and diffuse reflectance spectroscopy. The compound crystallises in the monoclinic space group $P2_1/n$ with a = 7.9756(7), b = 10.5191(9), c = 25.880(2) Å and β = 90.864(5)°. Alternating SbS_3^{3-} trigonal pyramids and $Sb_3S_6^{3-}$ semi-cubes generate $Sb_4S_7^{2-}$ chains which are directly bonded to $Cr(tren)^{2+}$ pendant units. The effective magnetic moment of 4.94(6) μ_B shows a negligible orbital contribution, in agreement with expectations for Cr(II):d^4 in a ^{5}A ground state. The measured band gap of 2.14(3) eV is consistent with a correlation between optical band gap and framework density that is established from analysis of wide range of antimony sulphides.

Keywords:

A. Chalcogenides

B. Crystal growth

C. X-ray diffraction

D. Optical Properties

D. Magnetic Properties

Introduction

Template-directed synthesis is widely used in the preparation of novel chalcogenides [1,2]. Such new materials have the potential to exhibit interesting electrical, optical and magnetic properties [3]. Of particular interest are the antimony (III) sulphides which exhibit a wide structural diversity due to the stereochemical effect of the lone pair of electrons associated with Sb(III), and the ability of Sb(III) to adopt 3-fold and pseudo 4- and 5-fold coordination [4]. In solvothermally-synthesised antimony (III) sulphides, the primary building units are generally SbS_3^{3-} trigonal pyramids. These may be connected *via* corner- or edge-sharing to generate isolated molecular ions [5], chains [6], layers [7] and three-dimensional structures [8]. The $Sb_4S_7^{2-}$ chain, which is comprised of alternating $Sb_3S_6^{3-}$ semicubes and SbS_3^{3-} trigonal pyramids, is particularly prevalent. Such chains may occur in isolation, with individual chains separated by template molecules [9,10,11], or may be bridged *via* shared sulphur atoms, persulphide linkages or $Sb_2S_4^{2-}$ units to form double chains of stoichiometry $Sb_8S_{14}^{2-}$ [12], $Sb_8S_{13}^{2-}$ [13], or $Sb_{10}S_{16}^{2-}$ [14] respectively.

The introduction of a transition-metal cation into the synthesis mixture usually leads to in-situ formation of a transition-metal-amine complex. This species in turn can act as a structure directing agent for the growth of anionic antimony-sulphide frameworks and additionally provide a charge balancing counter-ion to the anionic framework. For example, anionic SbS_2^- and $Sb_4S_7^{2-}$ infinite chains in $[M(en)_3]Sb_2S_4$ [M = Co, Ni, Fe] [6,11] and $[M(en)_3]Sb_4S_7$ [M = Co, Ni, Fe] [11,15] are charge-balanced by cationic tris(ethylenediamine) transition-metal complexes whilst bis(diethylenetriamine)-iron(II) complexes fulfil a similar rôle in $[Fe(detn)_2]Sb_6S_{10}.0.5H_2O$, which contains $Sb_6S_{10}^{2-}$ layers [7]. In $[Co(en)_3]Sb_{12}S_{19,}$ the anionic three-dimensional antimony-sulphide framework contains $Co(en)_3^{2+}$ cations within one-dimensional channels [16].

In a small number of examples, transition metals are directly coordinated to the primary-bonded antimony-sulphide framework through transition- metal-sulphur bonds. In the majority of cases, this is achieved through the use of an amine which does not fully coordinate the transition-metal cation, leaving vacant coordination sites to be occupied by transition-metal-sulphur bonds.

Tris(2-aminoethyl)amine (tren) is particularly useful in this respect as it has only four nitrogen donor atoms, leaving the transition-metal centre coordinatively unsaturated. Examples in which transition-metal-tren complexes are bonded directly to antimony-sulphide units include the discrete molecular units of $[Co(tren)]_2Sb_4S_8$ and $[Co(tren)]_2Sb_2S_5$, in which two $Co(tren)^{2+}$ cations are bridged *via* $Sb_4S_8^{4-}$ or $Sb_2S_5^{4-}$ units through cobalt-sulphur bonds [17]; $[Fe(tren)]FeSbS_4$ containing $Fe(tren)^{2+}$ cations bonded to $FeSbS_4^{2-}$ chains [18] and two-dimensional $[Co(tren)]Sb_2S_4$, in which antimony-sulphide sheets are connected to $Co(tren)^{2+}$ cations [19].

Here we describe the synthesis and characterisation of the first chromium(II)-antimony-sulphide, $[Cr(tren)]Sb_4S_7$. This material is isostructural with a series of transition-metal containing compounds synthesised by Schaefer *et al.* [20]. Magnetic properties indicate the presence of Cr(II) in an orbitally non-degenerate ground state, consistent with an unusual trigonal-pyramidal coordination geometry. The organically coordinated Cr(II) is attached to an antimony-sulphide backbone giving a relatively low-density chain-like structure, with an optical band gap of 2.14(3) eV. A linear relationship between optical band gap and antimony-sulphide framework density is also established in this work.

Experimental Section

$[Cr(tren)]Sb_4S_7$ was prepared under solvothermal conditions in a Teflon-lined stainless steel autoclave with an inner volume of 23 ml. A mixture of Sb_2S_3 (0.679 g, 2 mmol), Cr (0.104 g, 2 mmol) and 3 ml 50% aqueous tris(2-aminoethylamine) (tren, Aldrich) containing S (0.001 g, 0.03 mmol), with an approximate molar composition Sb:Cr:S:tren of 4:2:6:10, was thoroughly mixed, heated at 438 K for 21 days and cooled to room temperature at a cooling rate of 20 Kh^{-1}. The solid product was filtered, washed in distilled water then acetone and dried in air at room temperature. The product consisted of large orange plates of $[Cr(tren)]Sb_4S_7$ as the major component, together with a small amount of black polycrystalline powder identified by powder X-ray diffraction as consisting of a mixture of Cr_2S_3, Cr_5S_6 and unreacted Sb_2S_3. Combustion analysis of a handpicked

sample of the title compound gave C, 8.18 ; H, 2.00; N, 6.29 %; (calc. for [Cr(tren)]Sb_4S_7: C, 7.92; H, 1.99; N 6.16 %). Thermogravimetric analysis was performed using a DuPont Instruments 951 thermal analyser. Approximately 3.5 mg of finely ground hand-picked crystals were heated at a rate of 10 $Kmin^{-1}$under a flow of dry nitrogen over the temperature range 298-673 K. A single step weight loss of 16.13% was observed between 585 and 601 K. This weight change is consistent with the complete loss of the organic component (calculated 16.07%). Powder X-ray diffraction data showed that the residue is amorphous.

Single-crystal X-ray diffraction data for [Cr(tren)]Sb_4S_7 were measured at 100 K using a Bruker Nonius X8 Apex diffractometer with Mo-K_α radiation (λ = 0.71073 Å). Intensity data were processed using the Apex-2 software [21]. The structure was solved by direct methods using the program SIR-92 [22], which located all Cr, Sb and S atoms. Subsequent Fourier calculations and least-square refinements on *F* were carried out using the CRYSTALS program suite [23]. The C and N atoms of the amine were located in a difference Fourier map. Hydrogen atoms were placed geometrically on the C and N atoms after each cycle of refinement. In the final cycles of refinement, positional and anisotropic thermal parameters for all non-hydrogen atoms were refined. Crystallographic and refinement details are given in Table 1.

Magnetic susceptibility measurements were performed using a Quantum Design MPMS2 SQUID susceptometer. *Ca.* 10 mg of hand-picked crystals of the title compound were loaded into a gelatine capsule at room temperature and data were collected over the temperature range ($5 \leq T/K \leq 300$) after cooling in the measuring field of 1000 G. Data were corrected for the diamagnetism of the gelatine capsule and for intrinsic core diamagnetism. Diffuse reflectance data were measured over the frequency range 9 090-50 000 cm^{-1} using a Perkin Elmer, Lambda 35 UV/Vis spectrometer. $BaSO_4$ was used as a reference material. Measurements were made on *ca.* 10 mg of finely-ground hand-picked crystals of [Cr(tren)]Sb_4S_7 diluted with $BaSO_4$. The band gap was determined by applying the Kubelka-Munk function [24].

Results and Discussion

The local coordination and atom labelling scheme of $[Cr(tren)]Sb_4S_7$ is shown in Figure 1 and selected bond lengths, angles and valence sums are presented in Table 2. In the asymmetric unit, there are four Sb atoms, seven S atoms and one $Cr(tren)^{2+}$ cation, all of which occupy general positions. Each antimony, with the exception of Sb(2), is coordinated to three sulphur atoms at distances in the range 2.3825(10)-2.4879(9) Å, with approximately trigonal pyramidal geometry in which S-Sb-S angles lie between 80.49(3) and 99.80(3)^o. Sb(2) is coordinated by four sulphur atoms, in a [2 + 2] arrangement with two shorter and two longer Sb-S bonds, as has been observed in a number of related materials [25, 26, 27]. The bond-valence sums [28] are consistent with a formal oxidation state of +3 for each antimony atom, resulting in anionic $Sb_4S_7^{2-}$ chains. These chains consist of alternating $Sb_3S_6^{3-}$ semi-cubes and SbS_3^{3-} trigonal pyramids. The terminal sulphur atoms of the linking SbS_3^{3-} trigonal pyramids act as monodentate ligands to coordinate to $Cr(tren)^{2+}$ units, thus forming infinite $[Cr(tren)]Sb_4S_7$ chains directed along [100] (Figure 2). The chromium cation is coordinated by the four nitrogen atoms of the tren ligand and by the S(1) atom of the thioantimonate(III) chain in a distorted trigonal bipyramidal geometry. The Cr-S bond is of length 2.3895(10) Å, and the Cr-N bond lengths range from 2.135(3)-2.306(3) Å.

In common with the majority of antimony-sulphide materials, secondary Sb…S interactions are also present at distances 3.11 - 3.69Å, which are less than the sum of the van der Waals' radii of antimony and sulphur (3.8 Å) [29]. These include both intra- and inter-chain interactions. Interchain interactions between Sb(4) and the sulphur atoms S(2) and S(4), serve to link individual chains into buckled layers, which lie parallel to the (001) plane (Figure 3). Hydrogen bonding between the amine ligand and the sulphur atoms of adjacent layers provides additional bonding.

The magnetic susceptibility data for $[Cr(tren)]Sb_4S_7$ indicate paramagnetism (Figure 4). A Curie-Weiss expression was fitted to the data, over the temperature range 50-300 K, yielding a Curie constant of 3.05(7) cm^3 K mol^{-1} and a Weiss constant of θ = -5.46(5) K. The former corresponds to an effective magnetic moment of 4.94(6) μ_B. This value is in good agreement with

the spin-only magnetic moment of 4.90 μ_B calculated for a high-spin d^4 cation and indicates that the orbital contribution is small. This is consistent with the orbitally non-degenerate ^{5}A ground state expected for a high-spin d^4 cation in a trigonal bipyramidal geometry for which the spin-orbit coupling constant, λ, is small [30]. Effective magnetic moments for Cr(II) in this unusual coordination geometry have been reported to lie in the range 4.82 – 4.89 μ_B [31, 32].

The diffuse reflectance spectrum (Figure 5(a)) of [Cr(tren)]Sb_4S_7 shows an absorption edge, together with two weak transitions at 10 000 and 13 700 cm^{-1}. The latter arise from transitions from the ^{5}A ground state of the trigonal bipramidally-coordinated (D_{3h} symmetry) Cr^{2+}:d^4 ion to first and second ^{5}E excited states. The energies of these two transitions compare favourably with the values of 10 800 and 14 000 cm^{-1} determined experimentally and theoretically calculated by Deeth *et al.* for [Cr(Me_6tren)Br]Br [33]. By applying the Kubelka-Munk function [24], the band gap of [Cr(tren)]Sb_4S_7 is determined as 2.14(3) eV (Figure 5(b)), suggesting that this material is a semiconductor. The isostructural series of materials containing Mn, Fe, Co and Zn, have band-gap values in the range 2.04 to 3.11 eV [20].

It has been observed by Parise and Yo [9] that the colour of solvothermally-synthesised antimony sulphides is related to the density of the antimony-sulphide framework. Qualitatively, the colour variations suggest that the optical band gap is inversely related to the framework density. Here we have explored this correlation in a semi-quantitative fashion by examination of the existing literature on optical band gaps, supplemented by a series of diffuse reflectance measurements on systems with a variety of structural motifs and dimensionalities. All measurements of the diffuse reflectance spectra and the band-gap determinations were carried out as described above. In order to facilitate comparison between materials containing organic counter-ions and those in which charge balancing is provided by a cationic transition-metal complex, the presence of which affects the absolute density, we use the number of antimony metal atoms per 1000 $Å^3$ as a measure of the density. This is similar to the approach adopted in zeolite chemistry [34] and focuses on the antimony-sulphide network, which is the principal contributor to the band structure. Using this

approach, it is clear (Figure 6) that the condensed binary phase Sb_2S_3 has the highest framework density (16.4 Sb atoms/ 10^3 Å^3) and also the smallest measured optical band gap of 1.54(5) eV. At the other extreme, [Cr(tren)SbS_3], which consists of discrete neutral complexes, has a calculated network density of 2.86 Sb atoms/ 10^3 Å^3 and a measured band gap of 2.52(4) eV. The network density of [Cr(tren)]Sb_4S_7 reported here (7.37 Sb atoms/ 10^3 Å^3) is approximately mid-way between these two extremes and this material has a band gap intermediate between those of Sb_2S_3 and [Cr(tren)SbS_3]. Furthermore, by considering the available body of data (Figure 6) a linear correlation between framework density and optical band gap holds remarkably well for materials with a wide range of structures, regardless of the dimensionality of the antimony-sulphide framework. In general, increasing the dimensionality of the structure raises the framework density and decreases the band gap. One exception to this is [TH_2]Sb_4S_7 (T = 1,4,8,11-tetraazacyclotetradecane (cyclam)), which adopts a microporous open framework-type structure reminiscent of a zeolite [35]. Hence, despite the increased dimensionality, the framework has a very low density. Similarly, efficient packing of one-dimensional chains, as occurs in $[CH_3NH_3]_2Sb_8S_{14}$ [36] and $[C_2N_2H_{10}]Sb_8S_{13}$ [37], both of which contain double chains, can lead to higher than expected densities, with a concomitant reduction in the band gap.

The structure of the binary sulphide, Sb_2S_3, consists of double Sb_4S_6 chains of edge-linked SbS_5 square-based pyramids and SbS_3 trigonal pyramids. Band-structure calculations [38] indicate that the optical band gap in Sb_2S_3 corresponds to a transition between states of predominantly sulphur 3*p*-character in the lower valence band and states in the upper conduction band deriving from admixture of Sb 5*s*/p-type levels with sulphur *p*-levels. Furthermore, X-ray photoelectron spectroscopy [39] reveals that the highest energy valence-band levels of Sb_2S_3 derive from sulphur 3*p* lone pairs. A valence band of predominantly sulphur character separated by a band gap from a conduction band mainly of antimony character appears to be preserved in more complex quaternary antimony sulphides [40]. This suggests that despite the structural differences between the phases included in Figure 6, we may associate the optical band gap in these materials with a transition from

valence band levels of sulphur 3*p* character. In Sb_2S_3, the levels closest to the Fermi energy arise from interaction of these sulphur 3*p* levels with antimony 5*s* levels. As the number of antimony centres per unit volume is decreased, these interactions are weakened, with the result that the tail on the low-binding energy side of the valence band is contracted. Therefore, whilst a full analysis of the band gap data presented here requires detailed band structure calculations to be performed for each of the materials, it appears that the reduction in band gap with decreasing framework density may be associated with narrowing of the conduction band due to decreased overlap of the sulphur lone pairs with antimony 5*s* levels.

Conclusions

The title compound, $[Cr(tren)]Sb_4S_7$, which is isostructural with $[M(tren)]Sb_4S_7$ (M = Mn, Fe, Co, Zn) [20], provides the first example of a chromium(II) antimony sulphide. The structural, magnetic and optical properties of the compound are consistent with the presence of chromium as a high-spin Cr^{2+}:d^4 ion in trigonal bipyramidal coordination geometry. This is a somewhat unusual oxidation state in which to find chromium, despite the reducing conditions used in the synthesis. Although chromium(II) has been observed previously in sulphur environments, *e.g.* in the binary phases CrS and Cr_3S_4 [41] and the ternary phases $BaCrS_2$ [42], $CrEr_2S_4$ [43], and CrV_2S_4 [41], the only reported condensed phase chromium-antimony sulphide, $CrSbS_3$ [44], contains chromium in the +3 oxidation state. Examples of chromium-containing antimony sulphides, prepared in the presence of organic amines under solvothermal conditions similar to those described here, have to date also been restricted to the Cr(III) oxidation state [38, 39]. It has also been established here, from analysis of data for a wide range of thioantimonates of differing dimensionality, that a linear relationship exists between band gap and framework density and that the band gap of the title compound is consistent with this observed correlation.

Acknowledgements

The authors acknowledge financial support from the UK EPSRC for a studentship for RJEL, and for a single-crystal diffractometer. Dr P. Vaqueiro is also thanked for access to the diffuse reflectance spectrometer.

References

[1] R.L Bedard, S.T. Wilson, L.D. Vail, J.M. Bennett, E.M. Flanigen, in: P.A. Jacobs, R.A. van Santen (Eds.), Zeolites: Facts, Figures, Future, Elsevier, Amsterdam, 1989.

[2] J. Li, Z. Chen, R.J. Wang, D.M. Proserpio, Coord. Chem. Rev. 190-192 (1999) 707.

[3] T. Jiang, A. Lough, G.A. Ozin, R.L. Bedard, R. Broach, J. Mater. Chem. 8 (1998) 721.

[4] W.S. Sheldrick, M. Wachold, Coord. Chem. Rev. 176 (1998) 211.

[5] R. Kiebach, F. Studt, C. Näther, W. Bensch, Eur. J. Inorg. Chem. (2004) 2553.

[6] R.J.E. Lees, A.V. Powell, A.M. Chippindale, Polyhedron 24 (2005) 1941.

[7] R. Stahler, C. Näther, W. Bensch, Eur. J. Inorg. Chem. (2001) 1835.

[8] P. Vaqueiro, A.M. Chippindale, A.V. Powell, Inorg. Chem. 43 (2004) 7963.

[9] J.B. Parise, Y. Ko, Chem. Mater. 4 (1992) 1446.

[10] W. Bensch, M. Schur, Z. Naturforsch. B 52 (1997) 405.

[11] H.O. Stephan, M.G. Kanatzidis, Inorg. Chem. 36 (1997) 6050.

[12] R.J.E. Lees, A.V. Powell, A.M. Chippindale, Acta Crystallogr., Sect C 61 (2005) m516.

[13] K. Tan, Y. Ko, J.B. Parise, Acta Crystallogr., Sect C 50 (1994) 1439.

[14] X.Q. Wang, Eur. J. Solid State Inorg. Chem. 32 (1995) 303.

[15] P. Vaqueiro, D.P. Darlow, A.V. Powell, A.M. Chippindale, Solid State Ionics 172 (2004) 601.

[16] P. Vaqueiro, A.M. Chippindale, A.V. Powell, Inorg. Chem. 43 (2004) 7963.

[17] R. Stahler, W. Bensch, J. Chem. Soc., Dalton Trans. (2001) 2518.

[18] R. Kiebach, W. Bensch, R.D. Hoffmann, R. Pottgen, Z. Anorg. Allg. Chem. 629 (2003) 532.

[19] R. Stahler, W. Bensch, Eur. J. Inorg. Chem. 12 (2001) 3073.

[20] M. Schaefer, R. Stahler, W.R. Kiebach, C. Näther, W. Bensch, Z. Anorg. Allg. Chem. 630 (2004) 1816.

[21] Apex-2 Software, Bruker-AXS, Madison, Wisconsin, USA, (2004).

[22] A. Altomare, G. Cascarano, C. Giacovazzo, A. Guangliardi, M. Burla, G. Polidori, M. Camalli, J Appl. Crystallogr., Sect. A 27 (1994) 435.

[23] D.J. Watkin, C.K. Prout, J.R. Carruthers, P.W. Betteridge, CRYSTALS, ISSUE 10, Chemical Crystallography Laboratory, University of Oxford, UK, 1996.

[24] W.W. Wendlandt, H.G. Hecht, Reflectance Spectroscopy, Interscience Publishers, New York, 1966.

[25] L. Engelke, C. Näther, W. Bensch, Eur. J. Inorg. Chem. (2002) 2936.

[26] K. Volk, P. Bickert, R. Kolmer, H. Schäfer, Z. Naturforsch, B 34 (1979) 380.

[27] X. Wang, F. Liebau, J. Solid State Chem. 11 (1994) 385.

[28] N.E. Breese, M. O'Keeffe, Acta Crystallogr., Sect. B 47 (1991) 192.

[29] A. Bondi, J. Phys. Chem. 68 (1964) 441.
[30] J.S. Wood, J. Chem. Soc. A (1969) 1582.
[31] M. Ciampolini, Chemical Society: Chemical Communication 2 (1966) 47.
[32] F. Mani and P. Stoppioni, Inorg. Chim. Acta, 16 (1976) 177.
[33] R.J. Deeth, M. Gerloch, Inorg. Chem. 24 (1985) 4490.
[34] Ch. Baerlocher, W.M. Meier and D.H. Olson (Eds), Atlas of Zeolite Framework Types, 5th edition, Elsevier, Amsterdam, 2001
[35] A.V. Powell, R.J.E. Lees and A.M. Chippindale, Inorg. Chem., 45 (2006) 4261.
[36] R.J.E. Lees, A.V. Powell and A.M. Chippindale, Acta Crystallogr. Section C 61 (2005) m516.
[37] K. Tan, Y. Ko and J.B. Parise, Acta Crystallogr. Section C 50 (1994) 1439.
[38] A.G. Khasabov and I.Y Nikiforov, Sov. Phys. - Cryst. 16, (1971) 28.
[39] P.E. Lippens, J. OlivierFourcade, J.C. Jumas, A. Gheorghiu, S. Dupont and C Sénémaud, Phys. Rev. B 56 (1997) 13054.
[40] B. Deng, G.H. Chan, D.E. Ellis, R.P. Van Duyne and J.A. Ibers, J. Solid State Chem., 178 (2005) 3169.
[41] A.V. Powell, D.C. Colgan, P. Vaqueiro, J. Mater. Chem. 9 (1999) 485.
[42] O. Fuentes, C. Zheng, C.E. Check, J. Zhang, G. Chacon, Inorg. Chem. 38 (1999) 1889.
[43] A. Tomas, R. Chevalier, P. Laruelle, B. Bachet, Acta Crystallogr. Sect B 32 (1976) 3287.
[44] S. Jobic, P. le Boterf, F. Bodenan and G. Ouvrard, C.R. Acad. Sci. Paris 318 (1994) 893.

Figure Captions

Figure 1	Local coordination of [Cr(tren)]Sb_4S_7, showing the atom labelling scheme and thermal ellipsoids at 50% probability.
Figure 2	View along [001] of the [Cr(tren)]Sb_4S_7 chains. *Key:* Antimony, large solid circles; sulphur, large open circles; Chromium, large shaded circles; carbon, small solid circles; nitrogen, small open circles.
Figure 3	View along [100] of [Cr(tren)]Sb_4S_7 chains joined by longer Sb…S interactions into layers. Unit cell outlined and longer inter chain bonds shown as narrow black lines. (Amine molecules omitted for clarity).*Key:* as for Figure 2.
Figure 4	Zero field cooled magnetic susceptibility data and inverse susceptibility data (inset) for [Cr(tren)]Sb_4S_7. The solid line shows the fit to the Curie-Weiss expression.
Figure 5	Diffuse reflectance spectrum of [Cr(tren)]Sb_4S_7, with the spectroscopic transitions described in the text marked. The inset shows the extrapolation through the linear portion of the band edge used to determine the band gap.
Figure 6	The relationship between the optical band gap and framework density for antimony sulphides. The data used to construct this figure, together with the corresponding references to the literature values are provided as supplementary information.

Table 1. Crystallographic Data for $[Cr(tren)]Sb_4S_7$

Formula	$[CrC_6N_4H_{18}]Sb_4S_7$
M_r	909.69
crystal habit	Orange plate
crystal dimensions/mm	0.14 × 0.04 × 0.01
crystal system	Monoclinic
space group	$P2_1/n$
T /K	100
a /Å	7.9756(7)
b /Å	10.5191(9)
c /Å	25.880(2)
β °	90.864(5)
V /Å^3	2171.0 (3)
Z	4
μ /cm^{-1}	6.070
ρ_{calc} /gcm^{-3}	2.783
measured data	65109
unique data	10140
observed data ($I \geq 3\sigma(I)$)	6148
R_{int}	0.04
no. parameters refined	199
$R(F)$	0.0247
$_wR(F)$	0.0273

Table 2. Selected bond lengths [Å], angles [°] and bond valences (v.u.) for the $Sb_4S_7^{2-}$ anion in $[Cr(tren)]Sb_4S_7$**.**

		ν^*
Sb(1)-S(3)	2.4622(9)	0.97
Sb(1)-S(2)	2.4270(9)	1.06
Sb(1)-S(1)	2.4126(9)	1.11
		3.14
Sb(2)-S(7)	2.7839(9)	0.41
Sb(2)-S(5)	2.4694(10)	0.95
Sb(2)-S(4)	2.4598(9)	0.97
Sb(2)-S(2)	2.6382(9)	0.60
		2.93
Sb(3)-S(6)	2.4386(9)	1.03
Sb(3)-S(4)	2.4879(9)	0.90
Sb(3)-S(3)	2.4798(9)	0.92
		2.85
Sb(4)-S(7)	2.3825(10)	1.20
Sb(4)-S(6)	2.4746(9)	0.94
Sb(4)-S(5)	2.4837(9)	0.91
		3.05

S(3)-Sb(1)-S(2)	97.18(3)
S(3)-Sb(1)-S(1)	96.59(3)
S(2)-Sb(1)-S(1)	99.06(3)
S(5)-Sb(2-S(4)	102.49(3)
S(5)-Sb(2)-S(2)	85.29(3)
S(4)-Sb(2)-S(2)	85.00(3)
S(7)-Sb(2)-S(5)	82.20(3)
S(7)-Sb(3)-S(6)	80.49(3)
S(7)-Sb(3)-S(4)	81.28(3)
S(6)-Sb(3)-S(4)	97.99(3)
S(7)-Sb(4)-S(6)	96.46(3)
S(7)-Sb(4)-S(5)	90.66(3)
S(6)-Sb(4)-S(5)	99.80(3)

*bond valences and their sums calculated using parameters from reference [28]

Figure1

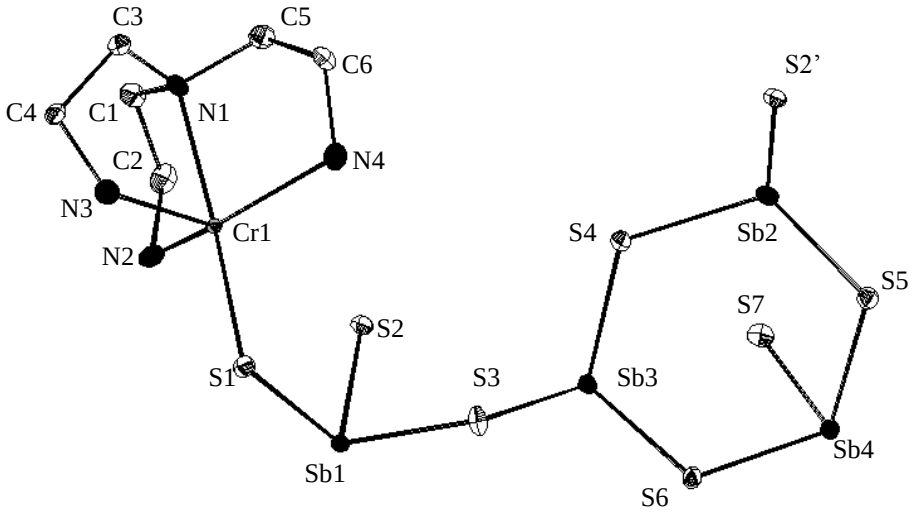
C3
C5
C6
S2'
C4
C1
N1
C2
N4
N3
Cr1
S4
Sb2
S5
N2
S7
S2
S1
S3
Sb3
Sb4
Sb1
S6

Figure2

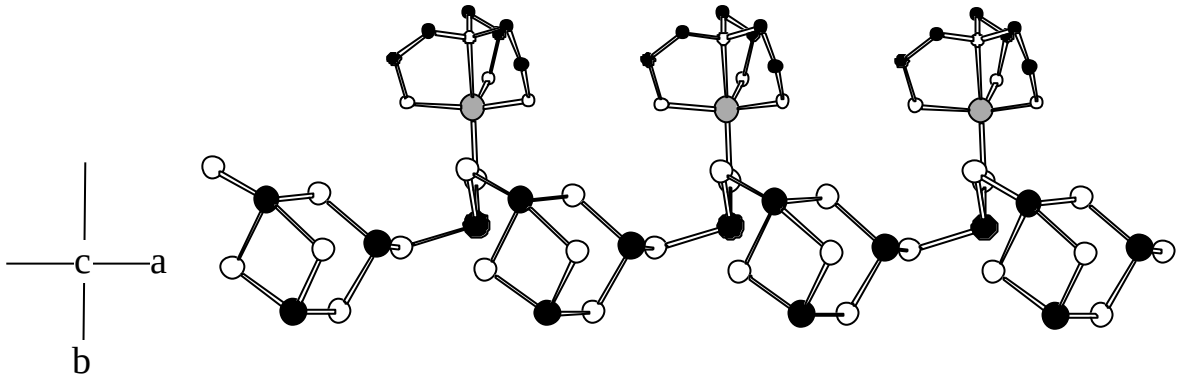

Figure 3

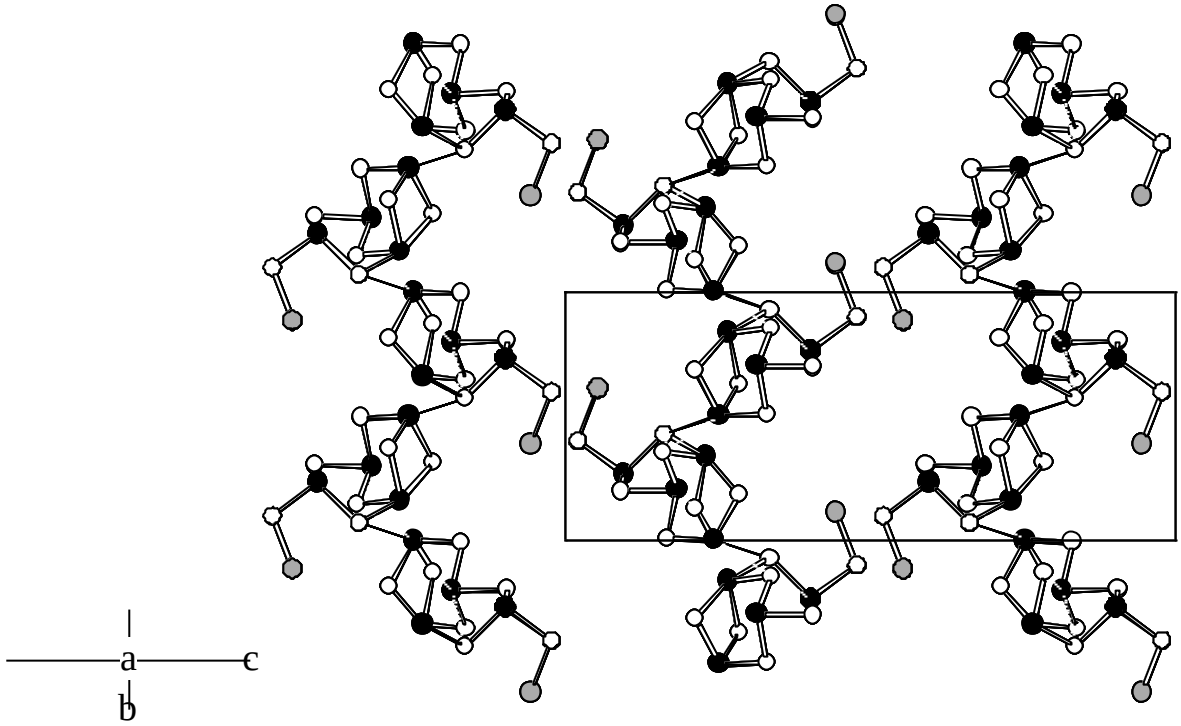

Figure 4

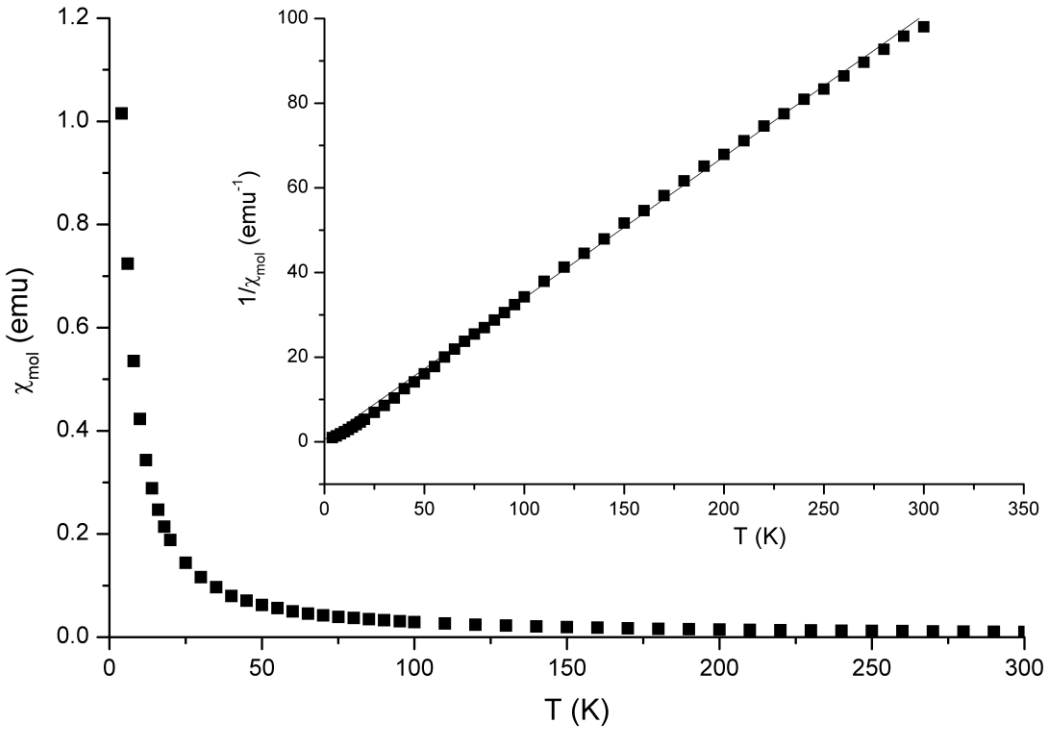
1.2
1.0
0.8
0.6
0.4
0.2
0.0
χmol (emu)
0
50
100
150
200
250
300
T (K)
100
80
60
40
20
0
1/χmol (emu-1)
0
50
100
150
200
250
300
350
T (K)

Figure 5

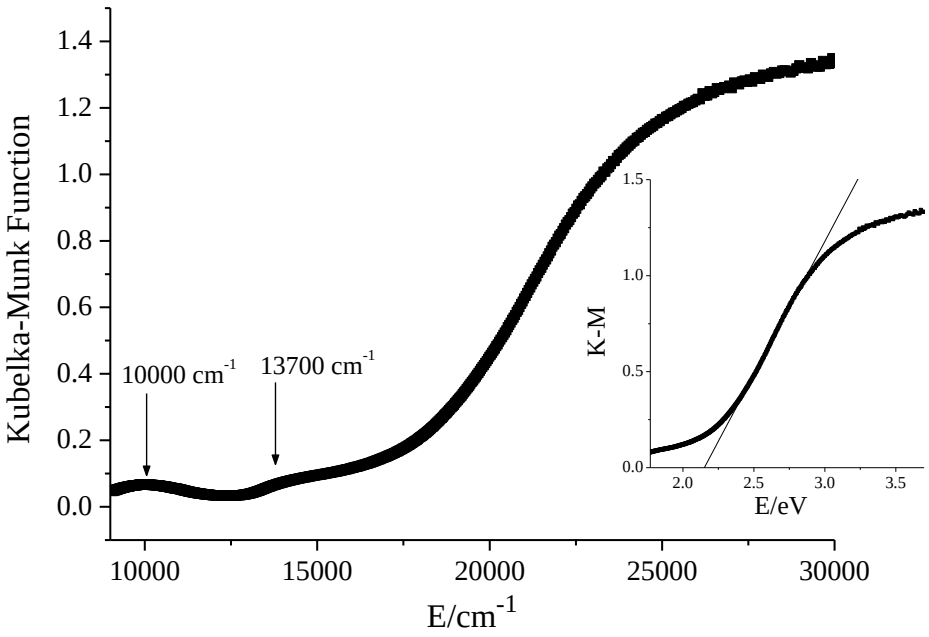

Figure 6

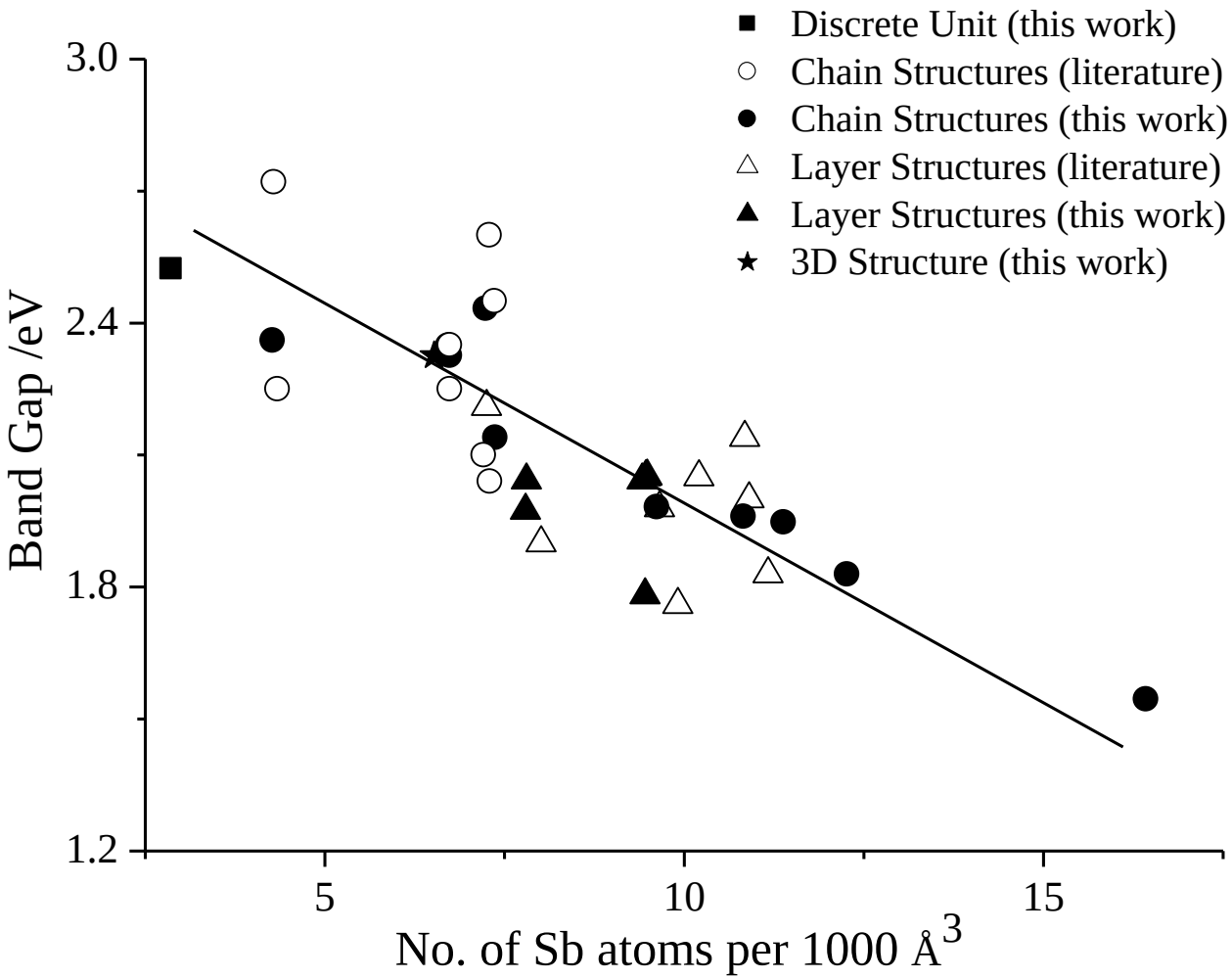
Discrete Unit (this work)
Chain Structures (literature)
Chain Structures (this work)
Layer Structures (literature)
Layer Structures (this work)
3D Structure (this work)
Band Gap /eV
3.0
2.4
1.8
1.2
5
10
15
No. of Sb atoms per 1000 Å3